

# Simulation of Ion Collection by a Sphere using the Particle-in-Cell Method on a GPU

by

Joshua Estes Payne

Submitted to the Department of Nuclear Engineering  
in partial fulfillment of the requirements for the degree of

Masters of Science in Nuclear Engineering

at the

MASSACHUSETTS INSTITUTE OF TECHNOLOGY

June 2012

© Massachusetts Institute of Technology 2012. All rights reserved.

Author .....  
Department of Nuclear Engineering  
May 18, 2012

Certified by .....  
Ian Hutchinson  
Associate Professor  
Thesis Supervisor

Accepted by .....  
Arthur C. Smith  
Chairman, Department Committee on Graduate Theses



# Simulation of Ion Collection by a Sphere using the Particle-in-Cell Method on a GPU

by

Joshua Estes Payne

Submitted to the Department of Nuclear Engineering  
on May 18, 2012, in partial fulfillment of the  
requirements for the degree of  
Masters of Science in Nuclear Engineering

## **Abstract**

In this thesis, I designed and implemented a compiler which performs optimizations that reduce the number of low-level floating point operations necessary for a specific task; this involves the optimization of chains of floating point operations as well as the implementation of a “fixed” point data type that allows some floating point operations to simulated with integer arithmetic. The source language of the compiler is a subset of C, and the destination language is assembly language for a micro-floating point CPU. An instruction-level simulator of the CPU was written to allow testing of the code. A series of test pieces of codes was compiled, both with and without optimization, to determine how effective these optimizations were.

Thesis Supervisor: Ian Hutchinson

Title: Associate Professor



# Acknowledgments

This is the acknowledgements section. You should replace this with your own acknowledgements.



# Contents

|          |  |           |
|----------|--|-----------|
| <b>1</b> | <b>Introduction</b>                                  | <b>17</b> |
| 1.1      | Motivation . . . . .                                 | 18        |
| 1.1.1    | GPUs vs CPUs . . . . .                               | 19        |
| 1.2      | Multiple Levels of Parallelism . . . . .             | 21        |
| 1.2.1    | Parallelization Opportunities in PIC Codes . . . . . | 21        |
| 1.2.2    | Current Status of GPU PIC codes . . . . .            | 21        |
| 1.3      | Overview of sceptic3D . . . . .                      | 21        |
| <b>2</b> | <b>Sceptic3D</b>                                     | <b>25</b> |
| 2.1      | Basic Code Structure . . . . .                       | 26        |
| 2.1.1    | Charge Assign Details . . . . .                      | 26        |
| 2.1.2    | Poisson Solve Details . . . . .                      | 26        |
| 2.1.3    | Particle Advancing Details . . . . .                 | 26        |
| 2.2      | CPU Code Profiling . . . . .                         | 26        |
| 2.3      | Overview of sceptic3Dgpu Goals . . . . .             | 26        |
| 2.3.1    | Main Routines . . . . .                              | 26        |
| 2.3.2    | Supporting Routines . . . . .                        | 26        |
| 2.3.3    | Challenges to overcome . . . . .                     | 26        |
| <b>3</b> | <b>Design Options</b>                                | <b>27</b> |
| 3.1      | Particle List Structure . . . . .                    | 27        |
| 3.1.1    | Other Codes . . . . .                                | 27        |
| 3.1.2    | In house tests . . . . .                             | 27        |

|          |  |           |
|----------|--|-----------|
| 3.2      | Charge Assign . . . . .                            | 27        |
| 3.2.1    | Naive Atomic Approach . . . . .                    | 27        |
| 3.2.2    | Other Codes . . . . .                              | 27        |
| 3.3      | Particle List Sort . . . . .                       | 27        |
| 3.3.1    | Costs and Benefits . . . . .                       | 27        |
| 3.3.2    | Other Codes . . . . .                              | 27        |
| 3.3.3    | In house tests . . . . .                           | 28        |
| 3.4      | Particle Advancing . . . . .                       | 28        |
| 3.4.1    | Assumptions . . . . .                              | 28        |
| 3.4.2    | Other Codes . . . . .                              | 28        |
| 3.4.3    | Reinjections and Diagnostics . . . . .             | 28        |
| 3.5      | Poisson Solve . . . . .                            | 28        |
| 3.5.1    | Desired Performance . . . . .                      | 28        |
| 3.5.2    | Performance vs Implementation Difficulty . . . . . | 28        |
| 3.6      | Grid Dimension Constraints and Handling . . . . .  | 28        |
| <b>4</b> | <b>Implementation</b>                              | <b>29</b> |
| 4.1      | Constraining Grid Dimensions . . . . .             | 29        |
| 4.1.1    | Constraints . . . . .                              | 29        |
| 4.1.2    | Holding to the constraints . . . . .               | 30        |
| 4.2      | Particle List Transpose . . . . .                  | 30        |
| 4.3      | Charge Assign . . . . .                            | 31        |
| 4.3.1    | Domain Decomposition . . . . .                     | 31        |
| 4.3.2    | Particle Bins . . . . .                            | 32        |
| 4.3.3    | Particle Push . . . . .                            | 33        |
| 4.4      | Particle List Sort . . . . .                       | 35        |
| 4.4.1    | Populating Key/Value Pairs . . . . .               | 35        |
| 4.4.2    | Sorting Key/Value Pairs . . . . .                  | 36        |
| 4.4.3    | Payload Move . . . . .                             | 36        |
| 4.5      | Poisson Solve . . . . .                            | 37        |



|          |   |           |
|----------|---|-----------|
| 4.6      | Particle List Advance . . . . .           | 37        |
| 4.6.1    | Checking Domain Boundaries . . . . .      | 38        |
| 4.6.2    | Diagnostic Outputs . . . . .              | 38        |
| 4.6.3    | Handling Reinjections . . . . .           | 38        |
| <b>5</b> | <b>Performance</b>                        | <b>39</b> |
| 5.1      | Test Setup . . . . .                      | 39        |
| 5.1.1    | Parameter Space Explored . . . . .        | 39        |
| 5.1.2    | Machine Parameters . . . . .              | 39        |
| 5.1.3    | Memory Bandwidth Comparison . . . . .     | 39        |
| 5.2      | Particle list size scan . . . . .         | 39        |
| 5.3      | Grid Size scan . . . . .                  | 50        |
| 5.3.1    | Absolute Size . . . . .                   | 50        |
| 5.3.2    | Ratio of Surface Area to Volume . . . . . | 50        |
| 5.4      | Kernel Parameters Scan . . . . .          | 50        |
| 5.5      | Discussion . . . . .                      | 50        |
| <b>6</b> | <b>Conclusion</b>                         | <b>51</b> |
| <b>A</b> | <b>Tables</b>                             | <b>53</b> |
| <b>B</b> | <b>Figures</b>                            | <b>55</b> |
|          | <b>Bibliography</b>                       | <b>59</b> |



# List of Figures

|     |  |    |
|-----|--|----|
| 1-1 | Flow schematic for the PIC method. Need to make figure . . . . .   | 18 |
| 1-2 | Performance comparison of GPUs vs CPUs. . . . .  | 20 |
| 1-3 | Multiple levels of parallelism. (1) Cluster of systems communicating through a LAN. (2) Multiple GPUs per system communicating through system DRAM. (3) Multiple streaming multiprocessors per GPU execute thread-blocks and communicate through GPU global memory. (4) Multiple cuda cores per multiprocessor execute thread-warps and communicate through on chip shared memory. . . . . | 22 |
| 1-4 | Flow schematic for the PIC method with parallelizable steps highlighted. Need to make figure . . . . .   | 23 |
| 2-1 | Flow schematic for the PIC method with sceptic subroutine names<br>Need to make figure . . . . .   | 26 |
| 4-1 | Graphical Representation of domain decomposition and ParticleBin organization. Need to make figure . . . . .   | 32 |
| 4-2 | Thrust Sort Setup and Call . . . . .   | 36 |
| 5-1 | Number of Particles Scan on a 128x64x64 grid . . . . .   | 40 |
| 5-2 | Number of Particles Scan on a 64x32x32 grid . . . . .  | 41 |
| 5-3 | Speedup factor Number of Particles Scan on a 128x64x64 grid . . . .  | 42 |
| 5-4 | Gridsize Scan with 8 million ptcls . . . . .   | 43 |
| 5-5 | Gridsize Scan with 8 million ptcls . . . . .   | 44 |
| 5-6 | Gridsize Scan with 16 million ptcls . . . . .  | 45 |

|      |   |    |
|------|---|----|
| 5-7  | Gridsize Scan with 16 million ptcls . . . . . | 46 |
| 5-8  | Gridsize Scan with 34 million ptcls . . . . . | 47 |
| 5-9  | Gridsize Scan with 34 million ptcls . . . . . | 48 |
| 5-10 | Sub Domain Size scan . . . . .                | 49 |
| B-1  | Armadillo slaying lawyer. . . . .             | 56 |
| B-2  | Armadillo eradicating national debt. . . . .  | 57 |

# List of Tables

|                          |    |
|--------------------------|----|
| A.1 Armadillos . . . . . | 53 |
|--------------------------|----|



# List of Algorithms

|     |  |    |
|-----|--|----|
| 4.1 | ParticleBin Bookmark Calculation . . . . . | 33 |
| 4.2 | GPU Charge Assign . . . . .                | 34 |
| 4.3 | Particle List Sort Overview . . . . .      | 35 |
| 4.4 | GPU Payload Move . . . . .                 | 37 |





# Chapter 1

## Introduction

Over the past century humanity has become increasingly dependent on the 4th state of matter, plasma. Attaining a better understanding of plasma behaviour and interaction is critical to developing faster computer chips, creating new sources of energy, and expanding humanities influence among the stars. One important subset of plasma behaviour is how plasmas interact with solid objects such as dust particles, probes, and bodies traveling through space. These interactions can be very difficult to explore experimentally, and therefore must be modelled.

A plasma's behaviour is heavily influenced by the collective electric and magnetic fields generated by the individual particles that comprise the plasma. This means that plasma behaviour is essentially a very large n-body problem, where for moderately dense plasmas n can be on the order of  $10^{20}$ . No computer currently in existence can store the information for  $10^{20}$  particles, and calculating the interaction of every particle in the set with every other particle would be prohibitively long. The solution to this problem is to model only a subset of the true number of particles. The modeled behaviour of these particles and their contributions to magnetic and electric fields can be used to statistically infer the behaviour of the rest of the plasma, essentially from first principles. This method is called particle-in-cell (PIC), and operates by moving particles on a potential grid and updating that potential with the new particle density at every timestep. The flow of a general PIC code is shown in figure 1-1. The PIC method is a very robust and straightforward scheme for modeling plasma behaviour,

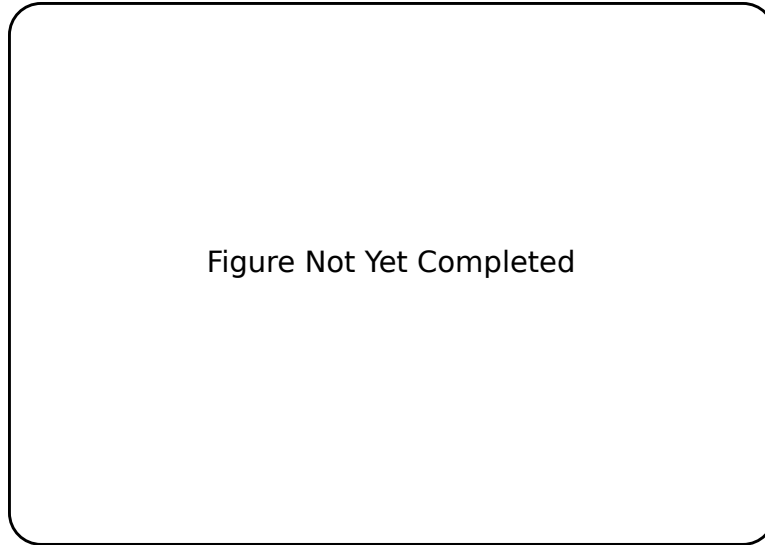


Figure 1-1: Flow schematic for the PIC method. Need to make figure

and is used extensively to model plasmas in complicated systems.

## 1.1 Motivation

The PIC method is very good at modeling complicated plasma behaviour, however this method still relies on tracking a very large number of particles for good statistics. In order to achieve “good” statistics PIC codes employ millions to billions of particles, which means that these codes can require a very large amount of computation time for each timestep. Running millions of particles on a single processor for hundreds of timesteps is not really feasible, it simply takes too long to compute a solution.

One way to reduce the total run time of PIC codes is to parallelize them. Since PIC codes operate on the fact that the potential changes little over the course of a single timestep, each particle can be assumed to be independent of its neighbors. This leads to a situation that is trivially parallel. In theory a machine with a million processors could run every particle on a separate processor. This is of course assuming that the majority of the computational complexity lies in moving the particles and that communication between processors is very fast.

### 1.1.1 GPUs vs CPUs

The ideal computing system for a particle in cell code should have a large number of relatively simple processors with very low communication costs. Traditional CPUs are just the oposite of this. CPUs tend to have 4-8 complicated processors that are very good at performing large operations on small sets of data, but very slow when it comes to communicating between multiple processors. CPUs are designed to be able to actively switch tasks on the fly. This makes them very good at simultaneously running web-browser, decoding a video, and playing a video game. However, this flexibility requires a large number of cycles to switch between tasks, and a large amount of cache to store partially completed tasks.

Graphical processing units, or GPUs, forgoe the flexibility of CPUs in favor of more raw processing capability. Reducing the size of the cache and employing single instruction multiple data (SIMD) parallelism allows GPU manufactures to combine hundreds of processors on a single chip. In order to supply enough data to keep hundreds of processors GPUs also have a very large data channel between the processors and DRAM. All of these features are chosen to create a math processor that excels at tasks where each processor operates on data that is invisible to the other processors. These features give GPUs a significant raw floating point performance advantage over CPUs as seen in figure 1-2.

The hardware in GPUs is tailored to excel at performing tasks such as ray-tracing, which is very similar to particle moving. Therefore it is by no means unreasonable to conclude that GPUs can be very good PIC code processors. The advantages that GPUs have over CPUs for scientific computing include:

- Higher performance per cost.
- Higher performance per watt.
- Easier to upgrade.
- GPUs still improving with Moore's law.

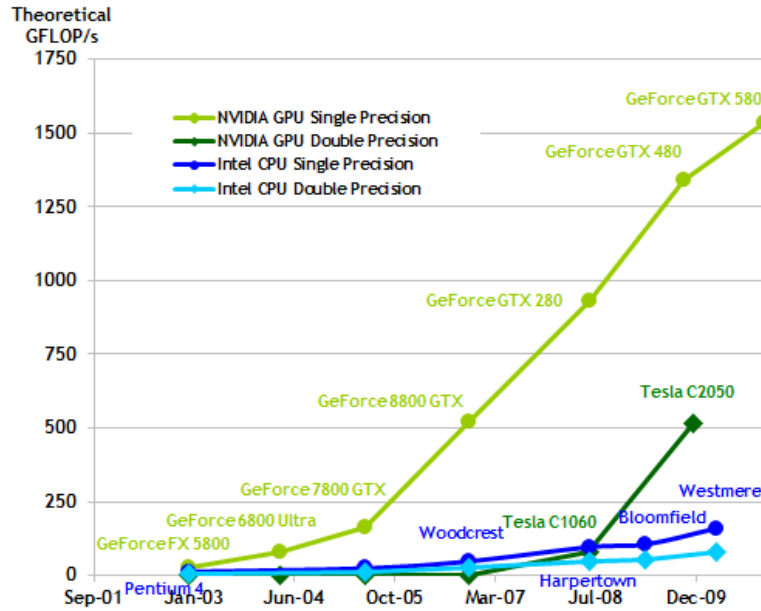


Figure 1-2: Performance comparison of GPUs vs CPUs.

All of which are observed when comparing the CPU and GPU versions of the same PIC code. While these advantages are very promising there are also several disadvantages to GPU computing:

- Increased code complexity.
- Smaller memory space.
- Smaller cache.
- Slow communication between CPU and GPU.
- Most developed GPU language is an extension of C.
- Algorithms can be very dependent on hardware configuration.

The key to developing efficient PIC algorithms that utilize GPUs lies in balancing the work between the two architectures. Some operations will be easier to implement on the CPU and be just as fast as the GPU while others will be significantly faster on the GPU. Partitioning the code between the different architectures begins to outline a very important aspect of parallel computing, multiple levels of parallelism.

## 1.2 Multiple Levels of Parallelism

Currently most parallelization is done by dividing up a task between a bunch of threads on different CPUs, and using an interface such as MPI to allow those threads to communicate. This network of threads has a master node, usually node 0, which orchestrates the communication between the other nodes. This is analogous to how a single CPU-GPU system operates. The CPU is the “Master” and serves as a communication hub for groups of execution threads on the GPU called thread blocks. Each thread block is itself a cluster of threads that can communicate through a memory space aptly named “shared memory”.

The point here is that multiple domain decompositions must be performed in order to fully utilize the capabilities of this system. The coarse decomposition is very similar to that used for MPI systems, but the fine decomposition can be very different due to the significantly higher memory bandwidth and smaller cache of GPUs.

### 1.2.1 Parallelization Opportunities in PIC Codes

### 1.2.2 Current Status of GPU PIC codes

Some work on efficient GPU based PIC codes has already been done. This past work will be briefly introduced here and discussed in depth in chapter 3. Bureau et al developed a fully relativistic PIC code for a gpu cluster.

## 1.3 Overview of sceptic3D

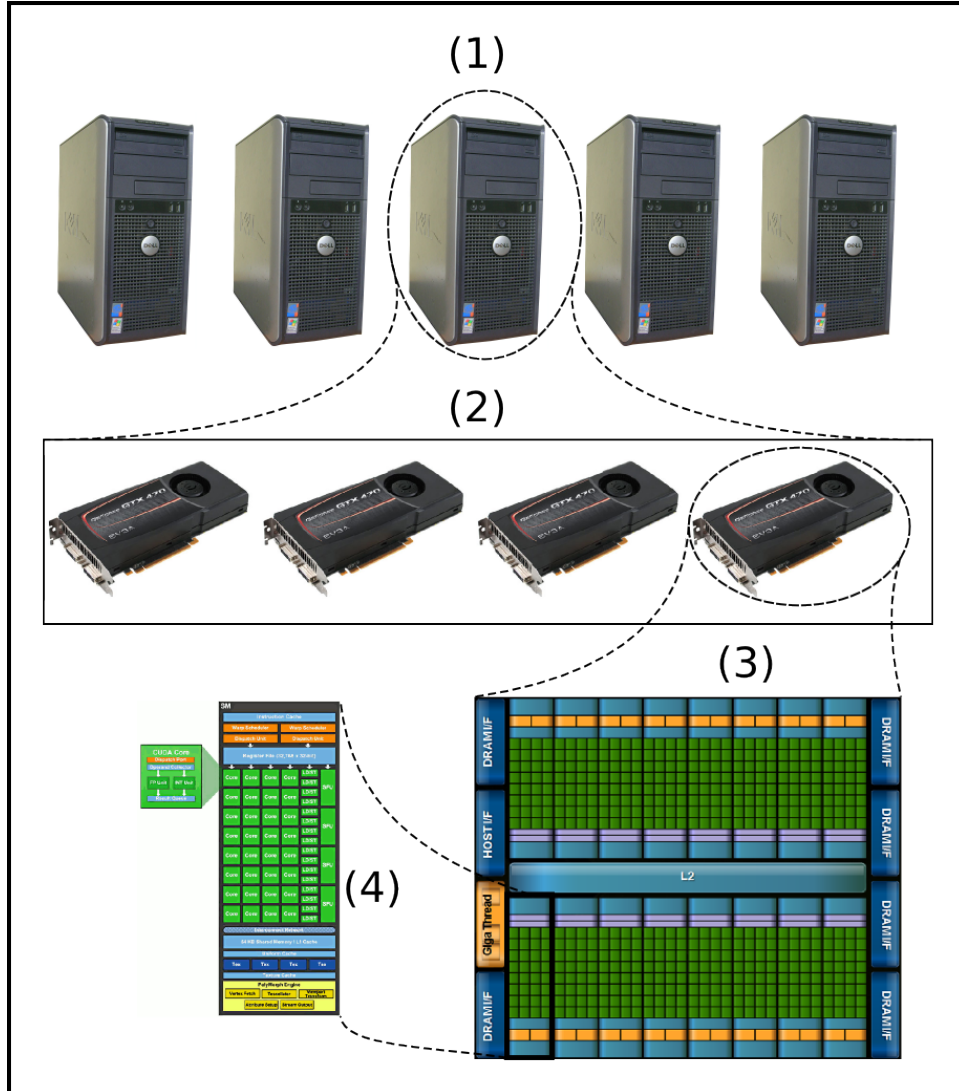


Figure 1-3: Multiple levels of parallelism. (1) Cluster of systems communicating through a LAN. (2) Multiple GPUs per system communicating through system DRAM. (3) Multiple streaming multiprocessors per GPU execute thread-blocks and communicate through GPU global memory. (4) Multiple cuda cores per multiprocessor execute thread-warps and communicate through on chip shared memory.

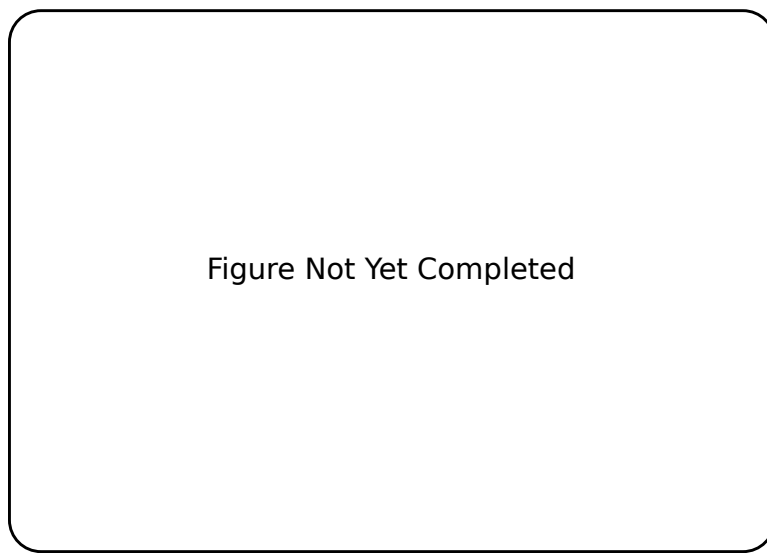


Figure 1-4: Flow schematic for the PIC method with parallelizable steps highlighted.  
Need to make figure





## Chapter 2

### Sceptic3D

Now that Sceptic3D is three dimensional hybrid PIC code specifically designed to solve the problem of ion flow past a negatively biased sphere in a uniform magnetic field. The current version of the code was derived from the 2D/3v code SCEPTIC which was originally written by Hutchinson [3, 4, 1, 2].

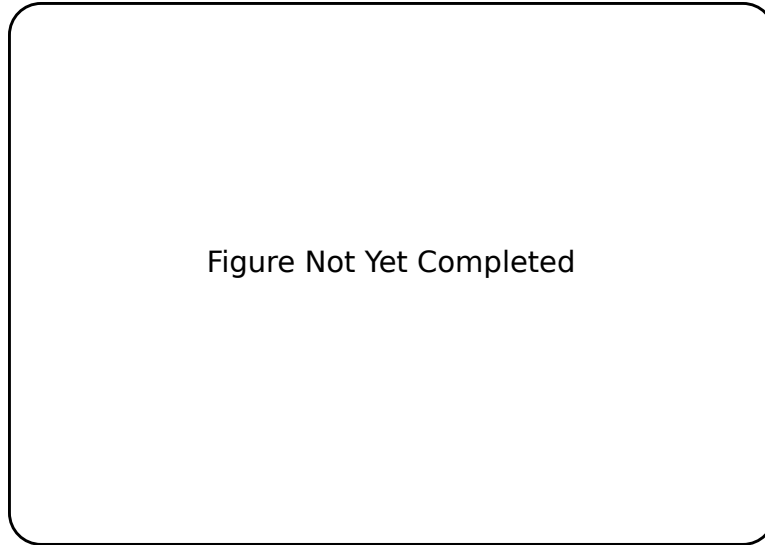


Figure 2-1: Flow schematic for the PIC method with sceptic subroutine names Need to make figure

## **2.1 Basic Code Structure**

### **2.1.1 Charge Assign Details**

### **2.1.2 Poisson Solve Details**

### **2.1.3 Particle Advancing Details**

## **2.2 CPU Code Profiling**

## **2.3 Overview of sceptic3Dgpu Goals**

### **2.3.1 Main Routines**

### **2.3.2 Supporting Routines**

### **2.3.3 Challenges to overcome**

# Chapter 3

## Design Options

### 3.1 Particle List Structure

#### 3.1.1 Other Codes

#### 3.1.2 In house tests

### 3.2 Charge Assign

#### 3.2.1 Naive Atomic Approach

#### 3.2.2 Other Codes

### 3.3 Particle List Sort

#### 3.3.1 Costs and Benefits

#### 3.3.2 Other Codes

\*Stantchev Particle Binning \*Kong Particle Passing \*Linked Particle List

### **3.3.3 In house tests**

## **3.4 Particle Advancing**

### **3.4.1 Assumptions**

### **3.4.2 Other Codes**

### **3.4.3 Reinjections and Diagnostics**

## **3.5 Poisson Solve**

### **3.5.1 Desired Performance**

### **3.5.2 Performance vs Implementation Difficulty**

## **3.6 Grid Dimension Constraints and Handling**

# Chapter 4

## Implementation

### 4.1 Constraining Grid Dimensions

#### 4.1.1 Constraints

There are two constraints that the grid dimensions must conform to. The first is set by the requirements of a simple z-order curve, the second is set by the size of the on chip shared memory. These constraints are expressed mathematically through the grid dimensions,  $n_r, n_\theta, n_\psi$ , and the block subdomain dimensions,  $nb_r, nb_\theta, nb_\psi$ .

$$\frac{n_r}{nb_r} = \frac{n_\theta}{nb_\theta} = \frac{n_\psi}{nb_\psi} = n_{virtual} \quad (4.1)$$

Where  $n_{virtual}$  is the number of blocks that the grid is divided into in any dimension. In order to fully satisfy the constraints for a simple z-order curve,  $n_{virtual}$  must be a power of 2.

The second constraint on the grid dimensions is set by the hardware. The goal is to maximize the shared-multiprocessor occupancy for the chargeassign stage of the code. Given that each block has the maximum number of threads, 512, and each thread requires roughly 25 registers, then the maximum number of threadblocks that can exist simultaneously on a single SM is 2. This means that each block can be allocated half of the total amount of shared memory on the SM. Compute capability 2.0 GPUs have 49152 bytes of shared memory per SM. Running two blocks per SM

provides each block with 24576 bytes of shared memory each, or 6144 floats per block. The maximum that all three block dimensions can be is 18. For the sake of simplicity this sets  $nb_r, nb_\theta$ , and  $nb_\psi \leq 18$ .

A third, loose constraint can be set in order to force a minimum number of thread-blocks for the charge-assign. The command line option “`–minbins#`” sets the parameter  $n_{virtual} = \#$ . This is useful in ensuring that enough threadblocks are launched to populate all of the SMs on the GPU. To populate all of the SMs on a GTX 470 the code would need to launch at least 28 thread-blocks. For a GTX 580 with 16 SMs 32 thread-blocks are required to fill all of the processors.

### 4.1.2 Holding to the constraints

## 4.2 Particle List Transpose

As previously mentioned the particle list structure on the GPU is different than the structure on the CPU. On the GPU particles are stored in a structure of arrays, while on the CPU they are stored in a  $6 \times n$  array. This means that in order to copy a particle list generated on the CPU to the GPU, or vice versa, the particle list must be transposed. The two main places in the code where this matters is when the particle list is initially populated at the start of the code, and when copying a list of pre-calculated reinjection particles from the CPU to the GPU at every time step during the advancing phase.

The particle list transpose was implemented on the CPU in two different ways depending on the compiler used and the available libraries. A GPU based particle list transpose is significantly faster than a CPU based transpose. However, the GPU has a very limited amount of DRAM compared to the CPU, and it is preferable to use as much of the available GPU memory as possible for the main particle list. In any case transposing the entire particle list only occurs once, but a smaller transpose is performed every time step for reinjected particles. This means that while a faster transpose is preferable, it represents so little of the total computation time that it is

not worth developing a complicated in place GPU transpose.

## 4.3 Charge Assign

As previously mentioned, the charge assign is one of the most difficult functions to parallelize. The naive approach of applying a thread to every particle and atomically adding each particle's contribution to an array in global memory is very slow. Grouping the particles spatially allows the majority of the atomic operations to be done in the context of shared memory which is much faster than global memory. The resulting algorithm resembles basic domain decomposition where each thread-block represents a separate sub-domain. The actual charge deposition method in this scheme is very similar to the naive approach, with a key difference being that all the threads in the thread block are operating on shared memory. Once all particles in the subdomain have contributed to grid in shared memory it takes only a small number of global memory accesses to write the contributions of a large number of particles to the main array  $\chi$ .

### 4.3.1 Domain Decomposition

The primary grid is decomposed into sub-domains of size  $nb_r, nb_\theta, nb_\psi$ . The methods for determining the size of the sub-domains is outlined in section ???. The indexing of the sub-domains is done using a z-order curve in order to preserve spatial locality of the sub-domains in memory. This is done in an attempt to reduce the mean distance that particles must be moved in memory during the sort phase. A graphical representation of this is shown in figure 4-1.

In addition to representing a sub-section of the computational mesh, each sub-domain must have a section of the particle list associated with it. The sub-domain must know all of the particles that reside within the region defined by that sub-domain. In essence each sub-domain represents a bin of particles that corresponds to some spatial location, hence the use of “ParticleBin” as the naming convention for these objects.

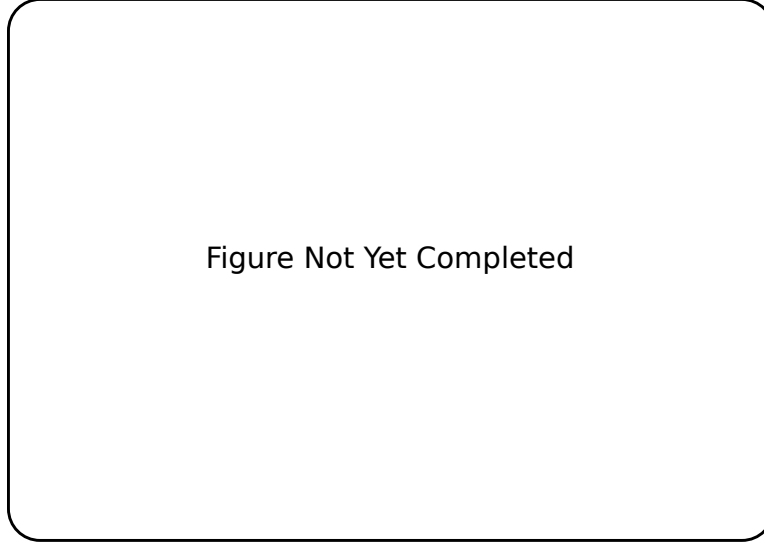


Figure 4-1: Graphical Representation of domain decomposition and ParticleBin organization. Need to make figure

### 4.3.2 Particle Bins

The *ParticleBin* object keeps track of all of the particles that reside in the region of space that the *ParticleBin* represents. For the sake of simplicity all of the particle bins are the same size spatially, which means that the *ParticleBin* object only has to keep track the section of the main particle list that the bin represents and the spatial origin of the bin.

In the context of the particle list each bin represents a pair of bookmarks that bound a section of the particle list. The bookmarks for each bin are calculated after the particle list is sorted by algorithm 4.1.

The spatial origin of the bin is hashed using a z-order curve and stored as a 16-bit unsigned-integer. This 16-bit integer is referred to as the binID and is used for determining the region of the domain that a bin is responsible for as well as a sorting key for the particle list. Calculating the binID will be discussed in more detail in section 4.4. A 16-bit unsigned integer is used for several reasons. First the sorting method detailed in section 4.4 is dependent on the number of bits of the sorting key. Second, the upper bound on the grid size set by using a 16-bit integer to store the z-order hash is much larger than the largest grid size that would need to be run. For



---

**Algorithm 4.1** ParticleBin Bookmark Calculation

---

**for all** threadID = 0  $\rightarrow$  ParticleList.nptcls in parallel **do**

```
    binID = ParticleList.binID[threadID]
    binIDleft = ParticleList.binID[threadID - 1]
    binIDright = ParticleList.binID[threadID + 1]
    if binID  $\neq$  binIDleft then
        ParticleBins[binID].ifirstp = threadID
        ParticleBins[binIDleft].ilastp = threadID - 1
    end if
    if binID  $\neq$  binIDright then
        ParticleBins[binID].ilastp = threadID
        ParticleBins[binIDright].ifirstp = threadID + 1
    end if
end for
```

---

a 16-bit integer this upper bound is  $512^3$  grid points. The third reason for using a 16-bit integer is that it also reduces the memory requirements of the particle list by about 5%, which does help when trying to run as many particles on the GPU as possible.

### 4.3.3 Particle Push

Now that the particles are organized spatially in memory, it is trivial to assign a single thread block to a region of space and corresponding particle bin in order to perform the particle push. This process is rather simple and is outlined in psuedo code in algorithm 4.2.

Each thread block reads in 512 particles at a time, although only 32 particles, a warp, are processed in parallel within the block. Each thread within this warp loops over the 8 nodes that bound the cell that contains the particle being processed. The nodes reside in a shared memory array, and are updated with the weighted particle data atomically. Once all of the nodes for a given particle have been updated the thread will retrieve a new particle from global memory. This process is repeated by all of the threads in the block until every particle in the particle bin has been processed. Once all of the particles have been processed the block then atomically updates the nodes in global memory with the values stored in shared memory.

---

**Algorithm 4.2** GPU Charge Assign

---

```
for all ParticleBin  $\in$  Grid in parallel do
  \ \ Inside the threadBlock with ID blockID
  __shared__ float subGrid(nbr, nb $\theta$ , nb $\psi$ )
  for all node  $\in$  subGrid in parallel do
    node = 0
  end for
  __syncthreads()
  for all particle  $\in$  ParticleBin in parallel do
    cell = particle.cell - ParticleBin.origin
    for all node  $\in$  cell do
      atomicAdd(subGrid(cell, node), weight(node))
    end for
  end for
  __syncthreads()
  \ \ Write block results to global memory
  for all node  $\in$  subGrid in parallel do
    atomicAdd(Grid(blockID, node), subGrid(node))
  end for
end for
```

---

The atomic operations in this algorithm lead to some very interesting time complexity behavior. In essence this algorithm is being executed on a machine with 32 processors. The time complexity of this scenario is  $\mathcal{O}(\frac{c}{p})$ , where  $c$  is constant and  $p$  is the number of available processors. When two processors attempt to atomically update the same memory address, one of the processors must wait until the other is finished. This means that one processor is effectively lost for a 1-way conflict.

The mean number of  $n$ -way atomic conflicts  $N$  in a warp over a sub domain of size  $G$ , and the execution time  $T$  is given by:

$$N = \frac{31!}{(31-n)!G^n} \quad T(n) \propto \frac{c}{32-n} \quad (4.2)$$

This means that the total time complexity of this algorithm with respect to the sub domain size  $G$  is:

$$T(G) \propto c \cdot \sum_{n=1}^{31} \frac{1}{32-n} \frac{31!}{(31-n)!G^n} \quad (4.3)$$

This behavior can be seen clearly in 5-10. This algorithm on the GPU can perform the particle push up to 200x faster than the CPU version of the charge assign. However, this algorithm relies on the particle data being ordered spatially, which contributes to the run time. The method used to maintain an ordered particle list on the gpu will be discussed in the following section.

## 4.4 Particle List Sort

As previously mentioned in section 4.3 an ordered particle list must be maintained in order for the charge assign to be fast. The particle list sort, algorithm 4.3 consists of three distinct subroutines, populating the key/value pairs, sorting the key/value pairs, and finally a payload move.

---

### Algorithm 4.3 Particle List Sort Overview

---

Populate\_KeyValues(Particles, Mesh, sort\_keys, sort\_values)

thrust::sort\_by\_key(sort\_keys,sort\_keys+nptcls,sort\_values)

Payload\_Move(Particles, sort\_values)

---

This method of maintaining particle list order was chosen because it is a good balance between simplicity and performance. An additional benefit of this routine is that it uses the sort from the thrust library, which is maintained by NVIDIA.

### 4.4.1 Populating Key/Value Pairs

The first step in sorting the particle list is ensuring that the key/value pairs needed by the sorting routine are populated. The sorting key for a particle is the index of the particle bin that the particle belongs to. Sorting values are simply the position of the particle in the unsorted list.

Calculating the particle bin index, or binid, begins with calculating the mesh cell that the particle resides in. This cell described by coordinates  $i_r, i_\theta, i_\phi$ . The coordinates of the particle bin that a given cell resides in is given by:

```

// wrap raw device pointers with a device_ptr
thrust::device_ptr<ushort> thrust_keys(binid);
thrust::device_ptr<int> thrust_values(particle_id);

// Sort the data
thrust::sort_by_key(thrust_keys, thrust_keys+nptcls, thrust_values);
cudaDeviceSynchronize();

```

Figure 4-2: Thrust Sort Setup and Call

$$ib_r = \frac{i_r}{nb_r}; \quad ib_\theta = \frac{i_\theta}{nb_\theta}; \quad ib_\phi = \frac{i_\phi}{nb_\phi} \quad (4.4)$$

The resulting block coordinates are then hashed using a z-order curve described in appendix A to give the binid. Each thread calculates the binid's for several particles and stores them in the sort\_keys array. Once a thread has calculated the binid for a particle it also stores the index of that particle as an integer in the sort\_values array.

#### 4.4.2 Sorting Key/Value Pairs

The key/value pair sorting is done using the thrust library sort\_by\_key template function. This function is provided by NVIDIA with CUDA. The thrust sort is a radix sort that has been optimized for NVIDIA GPUs[5]. The snippet of the sort code used in sceptic3Dgpu is shown in figure 4-2.

#### 4.4.3 Payload Move

The payload move is responsible for moving all of the particles from their old locations in memory to the new sorted locations. The idea is simple, each thread represents a slot on the sorted particle list. Threads read in an integer, the particleID, from the values array that was sorted using the binid's. This integer is the location of a given threads particle data in the unsorted list. Data at index particleID is read in, and stored in the new list at index threadID. While the idea is simple, this algorithm would require a completely separate copy of the particle list, a lot of wasted memory. However, since the particle list is set up as a structure of arrays, there is something that can be done to significantly reduce the memory requirements. The method,

outlined in algorithm 4.4 reorders only a single element of the particle list structure at a time.

---

**Algorithm 4.4** GPU Payload Move

---

```

for all member  $\in$  XPlist do
  float* idata = member
  float* odata = XPlist.buffer
  reorder_data(odata,idata,particleIDs)
  member = odata
  buffer = idata
end for

```

---

Essentially the idea is that a great deal of time and memory can be saved by statically allocating a “buffer” array that is the same size as each of the data arrays. During the payload move each data array is sorted into the buffer array. Some pointer magic is performed, the old buffer array becomes the new data array, and the old data array becomes the buffer for the next data array. For sceptic3Dgpu this implementation of the payload move only increases the particle list size by about 8.6%.

## 4.5 Poisson Solve

## 4.6 Particle List Advance

Moving the particles on the grid is fairly straightforward. The process starts with determining the acceleration of the particle. This is calculated by interpolating the potential,  $\phi$ , from the spherical mesh. The new position of the particle is simply  $\vec{x}' = \vec{x} + \vec{v}\Delta t + \frac{1}{2}\vec{a}\Delta t^2$ .

Implementing the particle advance on the GPU involved several interesting issues. Quickly determining whether a particle has crossed one of the domain boundaries, contributing to diagnostic outputs, and handling reinjections were the main issues.

**4.6.1    Checking Domain Boundaries**

**4.6.2    Diagnostic Outputs**

**4.6.3    Handling Reinjections**

# Chapter 5

## Performance

### 5.1 Test Setup

#### 5.1.1 Parameter Space Explored

#### 5.1.2 Machine Parameters

#### 5.1.3 Memory Bandwidth Comparison

### 5.2 Particle list size scan

The following tests were performed to explore the dependence of sceptic3Dgpu's runtime on the number of particles per node. These tests were performed using two MPI nodes and a grid size of 128x64x64.

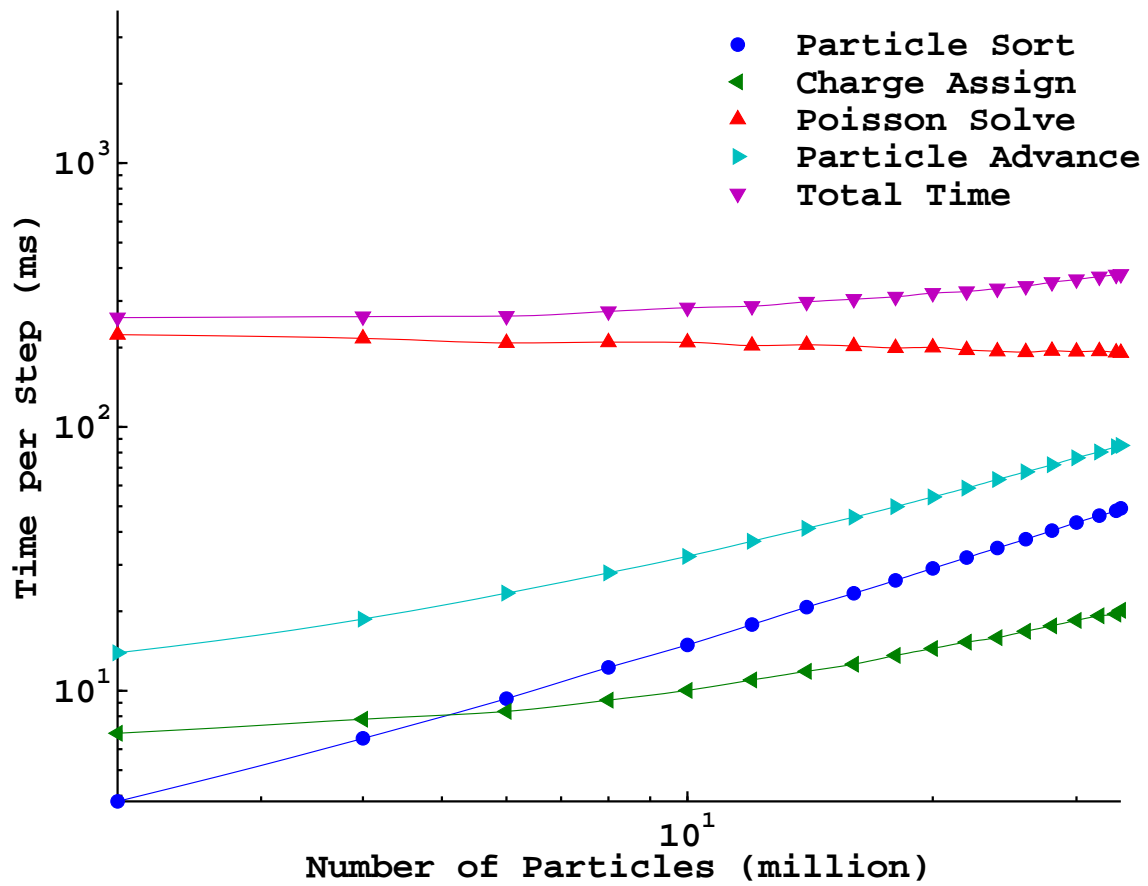


Figure 5-1: Number of Particles Scan on a 128x64x64 grid



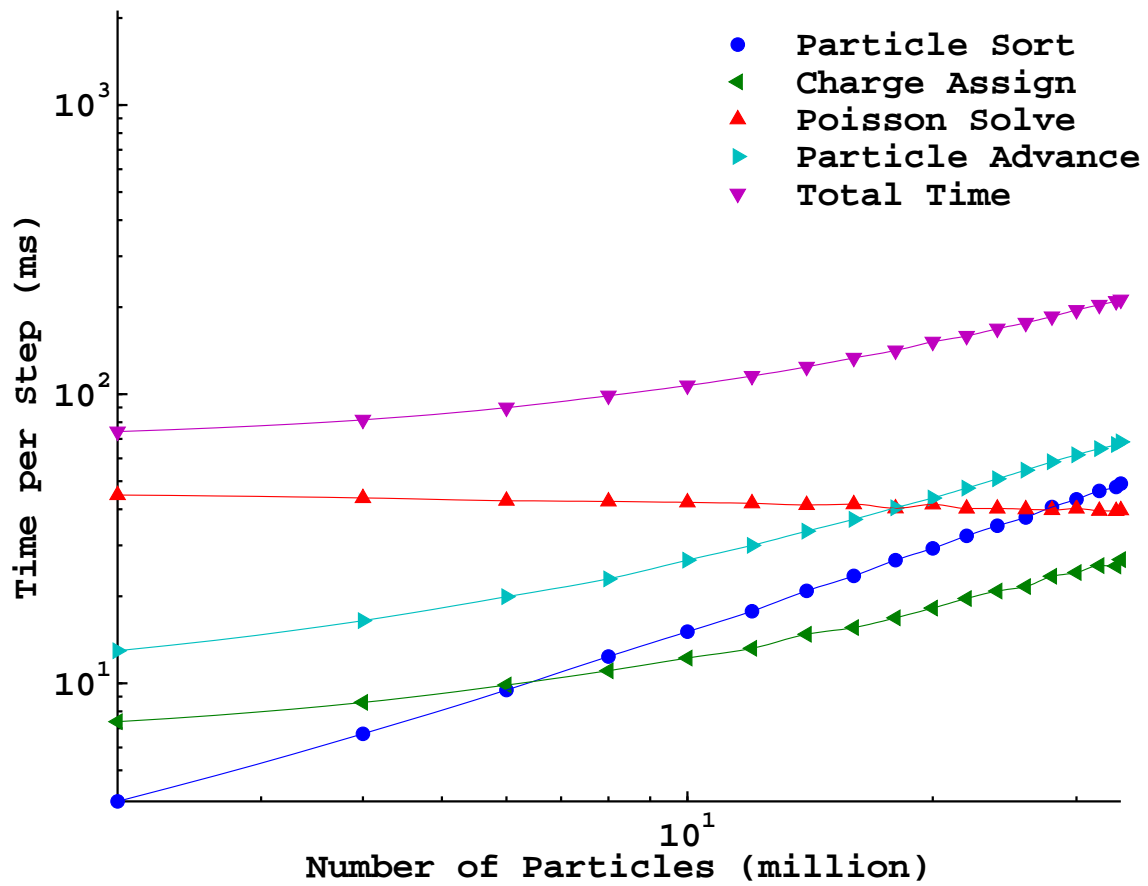


Figure 5-2: Number of Particles Scan on a 64x32x32 grid

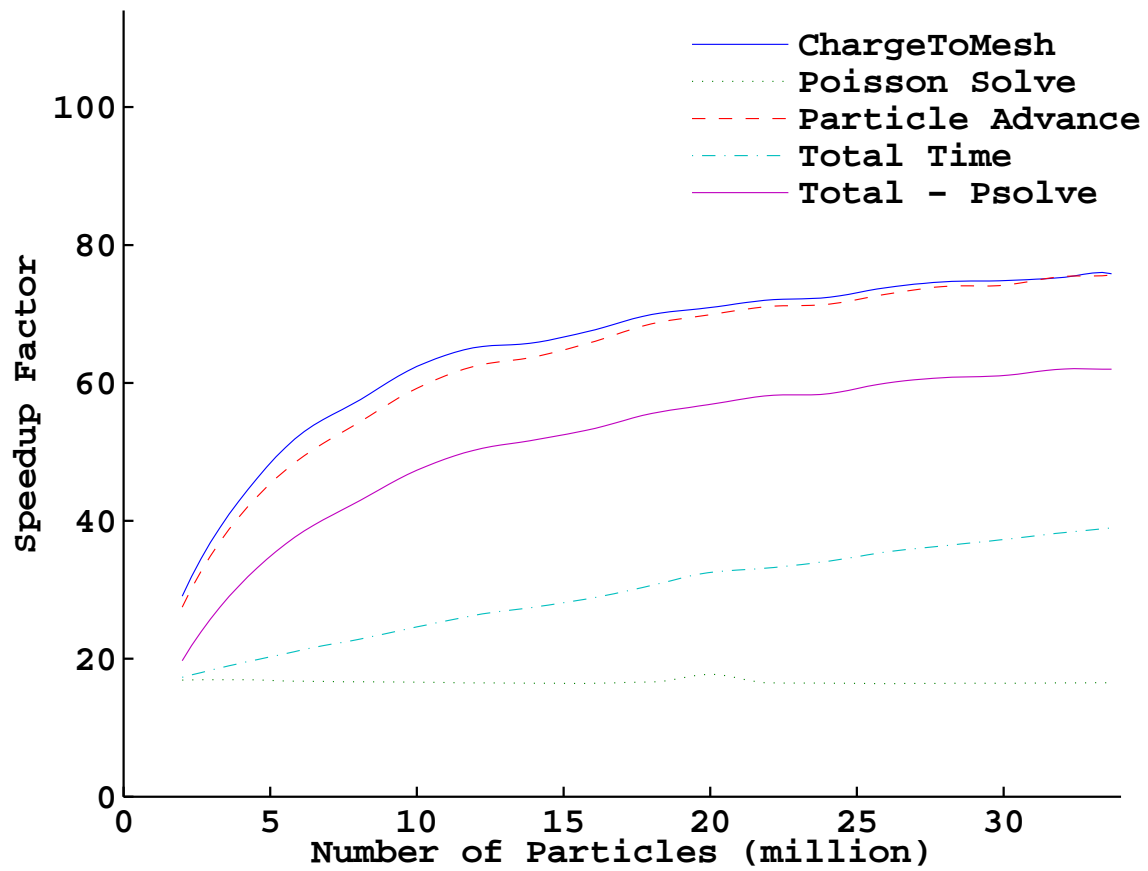


Figure 5-3: Speedup factor Number of Particles Scan on a 128x64x64 grid

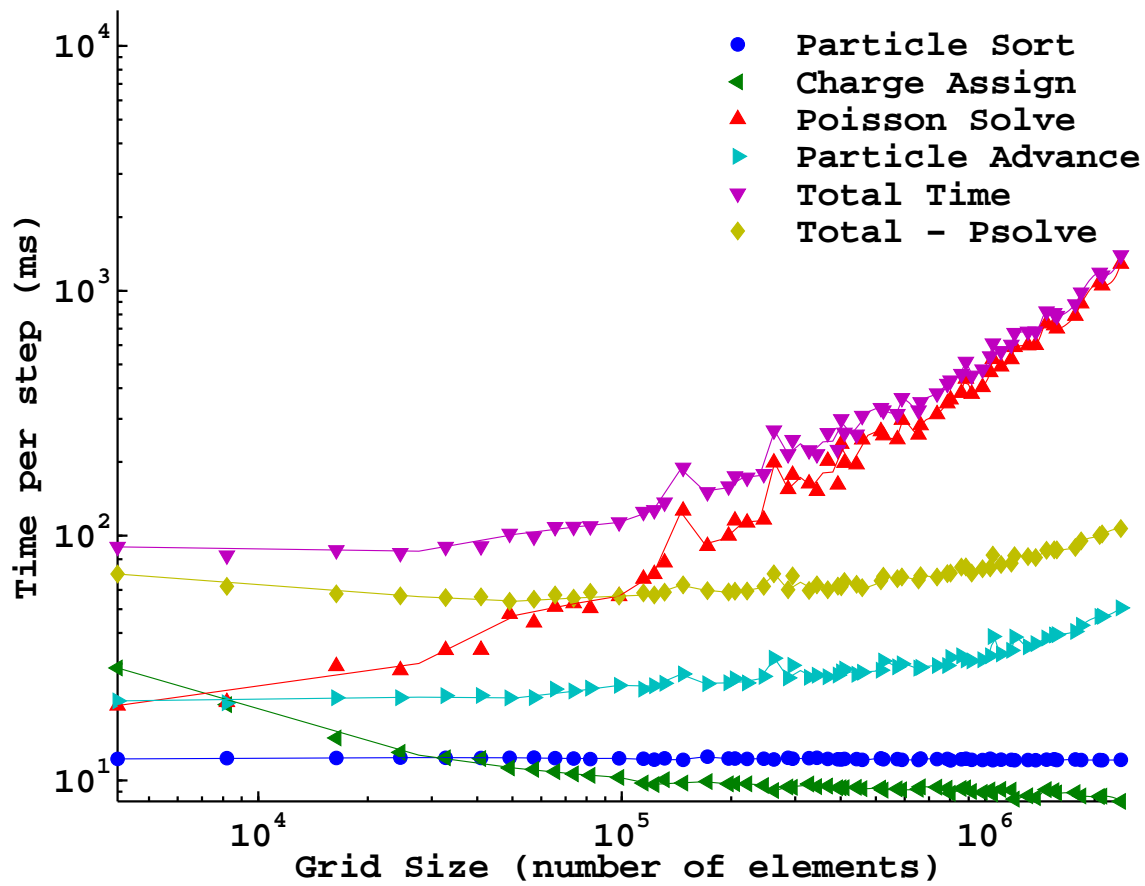


Figure 5-4: Gridsize Scan with 8 million ptcls

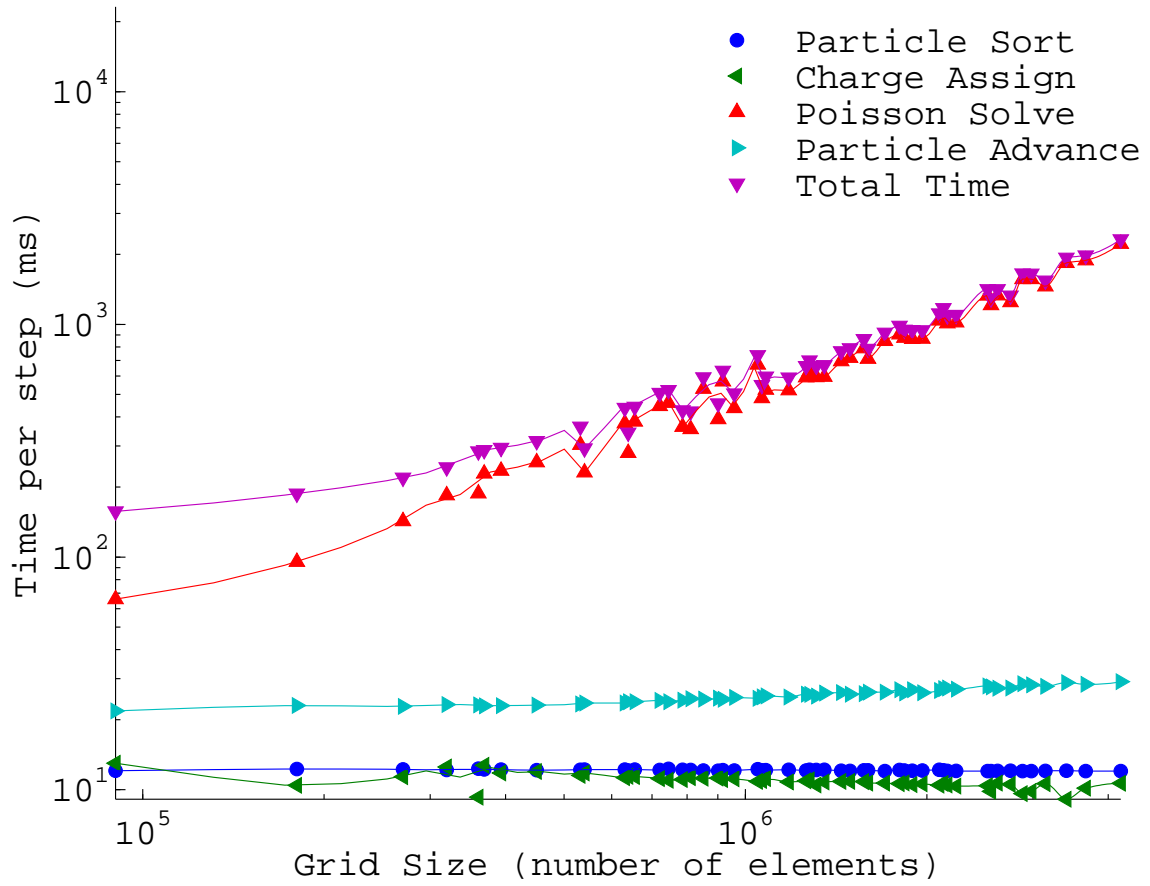


Figure 5-5: Gridsize Scan with 8 million ptcls

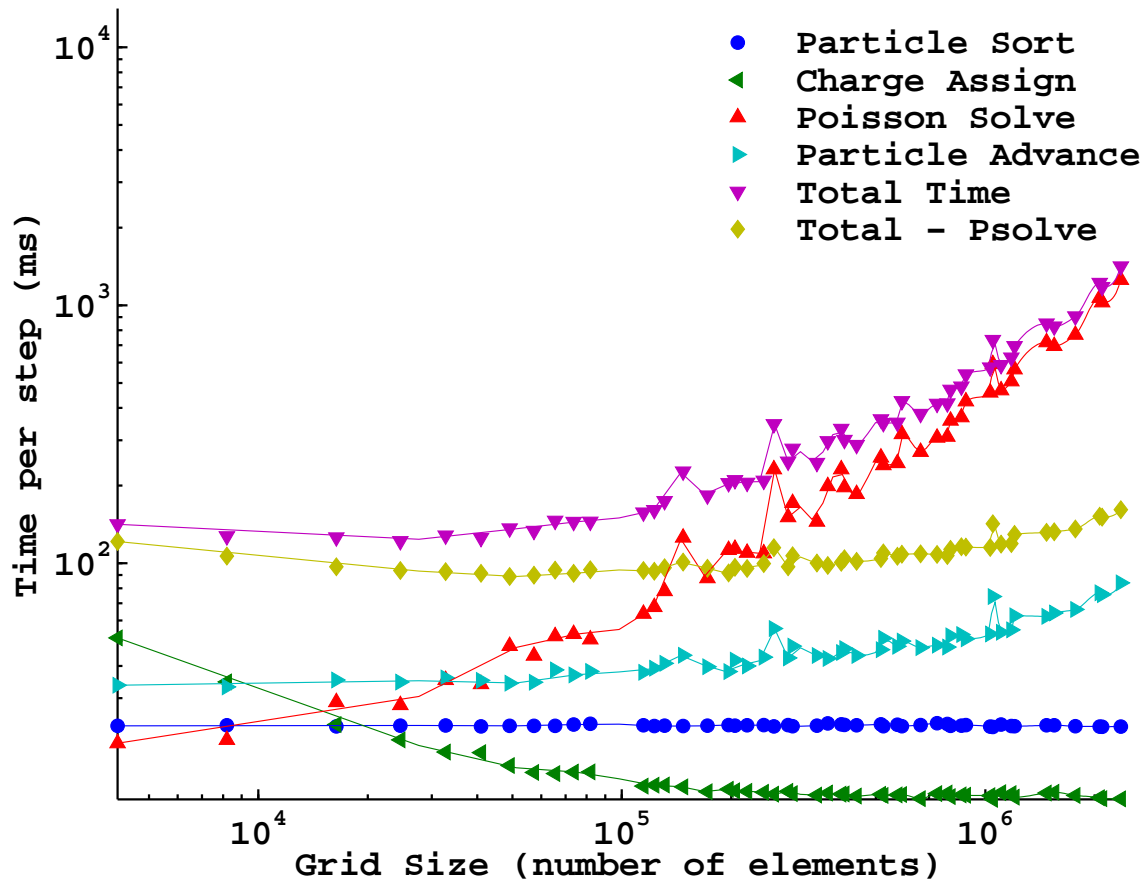


Figure 5-6: Gridsize Scan with 16 million ptcls

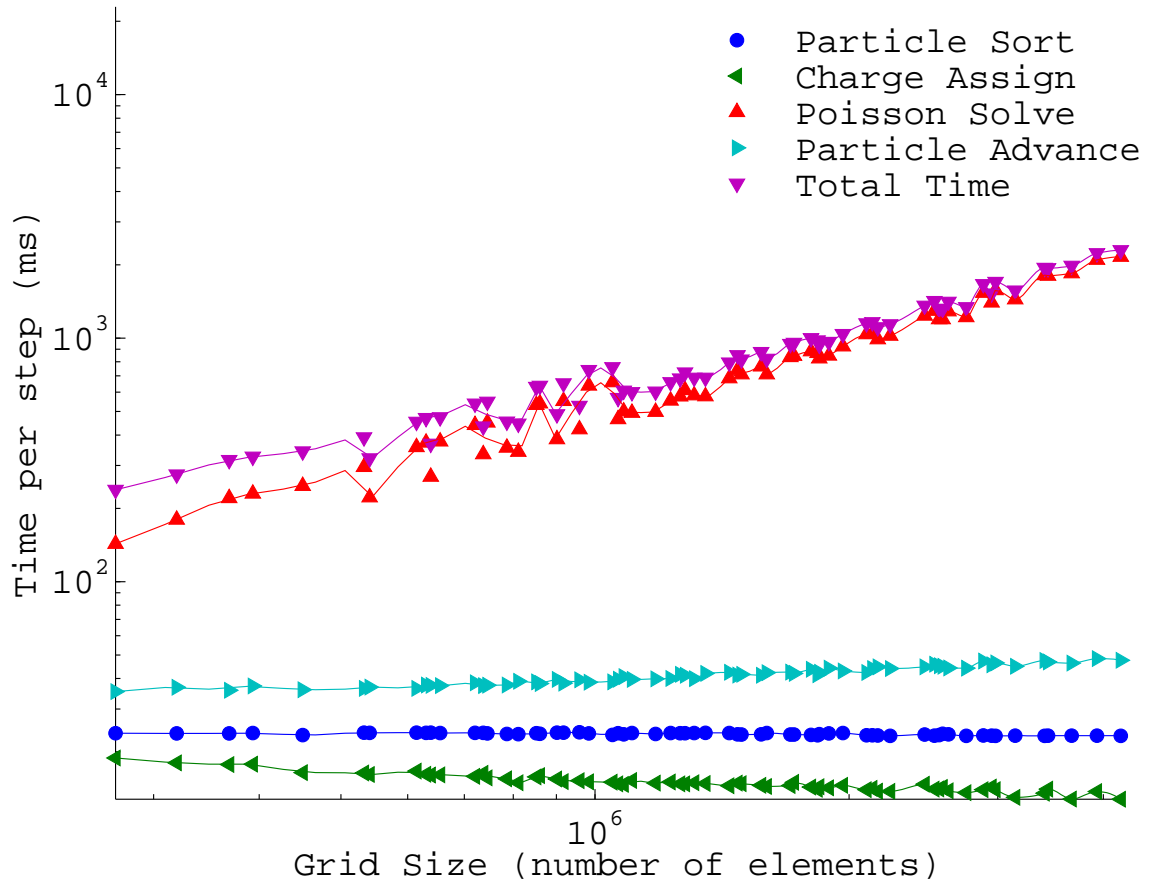


Figure 5-7: Gridsize Scan with 16 million ptcls

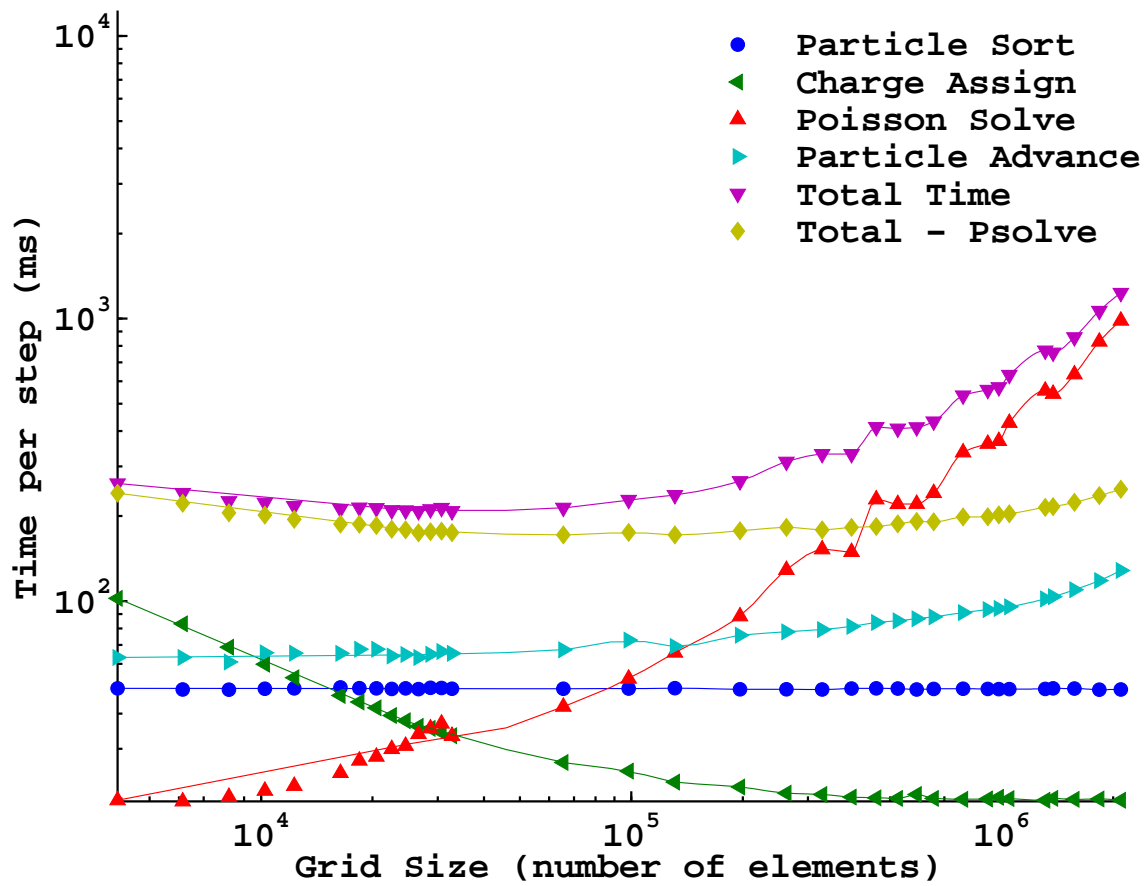


Figure 5-8: Gridsize Scan with 34 million ptcls

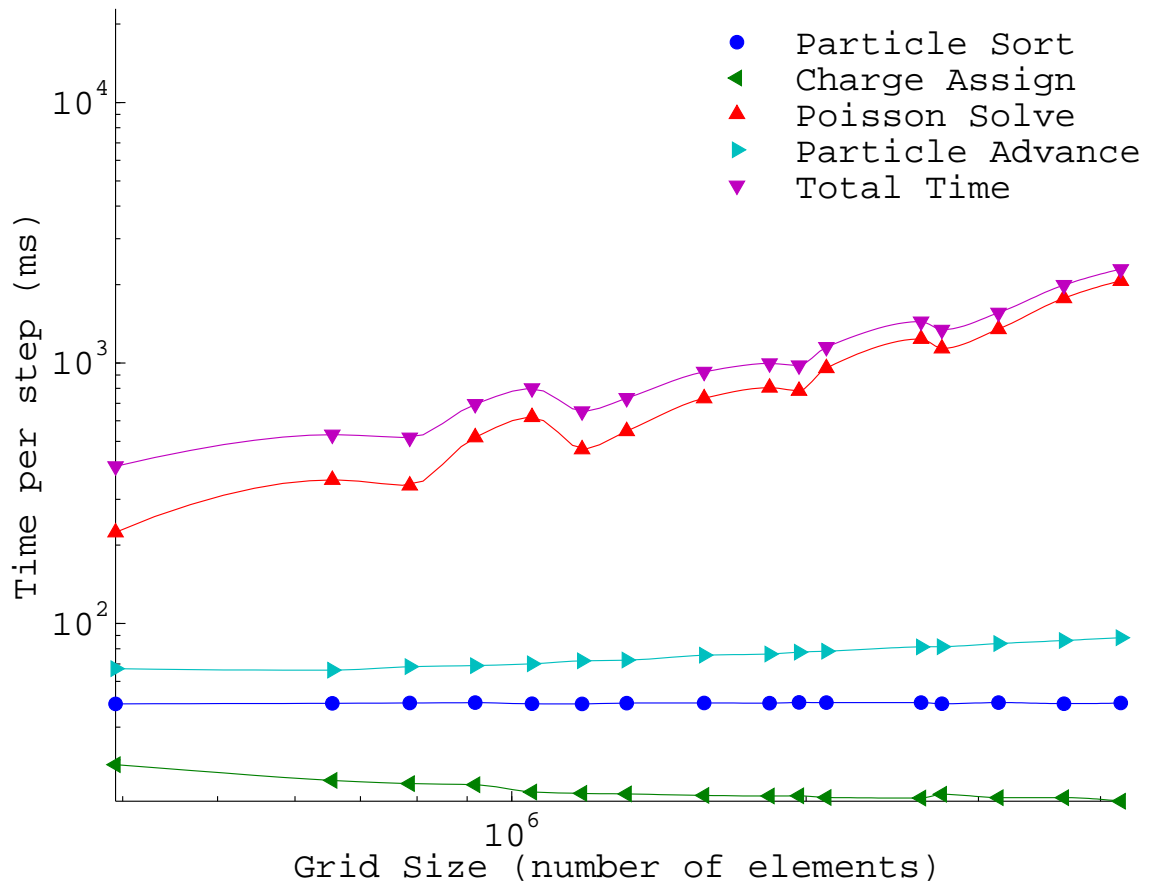


Figure 5-9: Gridsize Scan with 34 million ptcls



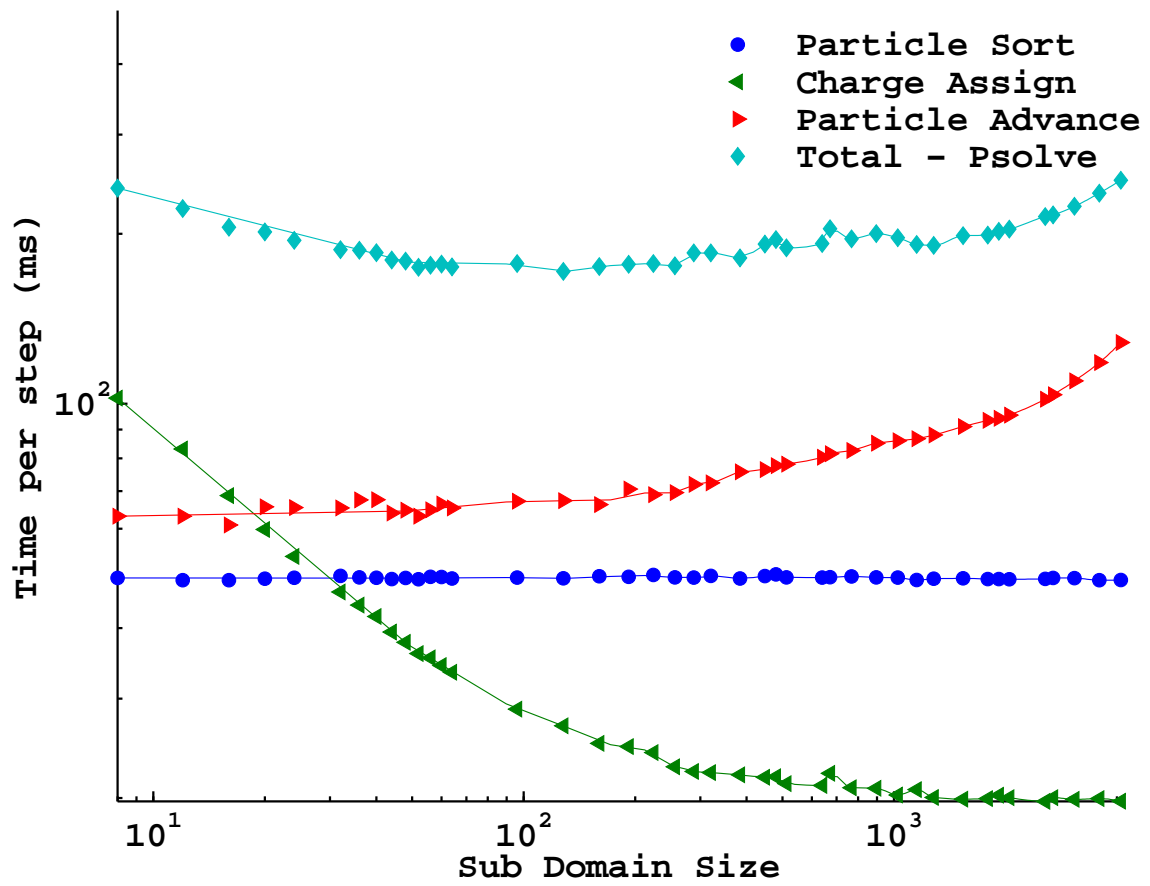


Figure 5-10: Sub Domain Size scan

## **5.3 Grid Size scan**

### **5.3.1 Absolute Size**

### **5.3.2 Ratio of Surface Area to Volume**

Global Domain Ratio

Threadblock Sub-Domain Ratio

## **5.4 Kernel Parameters Scan**

## **5.5 Discussion**

## Chapter 6

## Conclusion



# Appendix A

## Tables

Table A.1: Armadillos

|            |         |
|------------|---------|
| Armadillos | are     |
| our        | friends |



# Appendix B

## Figures

Figure B-1: Armadillo slaying lawyer.



Figure B-2: Armadillo eradicating national debt.



# Bibliography

- [1] I H Hutchinson. Ion collection by a sphere in a flowing plasma: 3. Floating potential and drag force. *Plasma Physics and Controlled Fusion*, 47(1):71–87, January 2005.
- [2] I H Hutchinson. Collisionless ion drag force on a spherical grain. *Plasma Physics and Controlled Fusion*, 48(2):185–202, February 2006.
- [3] IH Hutchinson. Ion collection by a sphere in a flowing plasma: I. Quasineutral. *Plasma physics and controlled fusion*, 1953, 2002.
- [4] IH Hutchinson. Ion collection by a sphere in a flowing plasma: 2. Non-zero Debye length. *Plasma physics and controlled fusion*, 1477, 2003.
- [5] NVIDIA Corporation. Thrust Quick Start Guide. Technical Report January, 2011.